Nuclear Engineering and Technology 55 (2023) 1593–1603

Contents lists available at ScienceDirect

Nuclear Engineering and Technology

journal homepage: www.elsevier.com/locate/net

Original Article

Development of transient Monte Carlo in a fissile system with β-delayed emission from individual precursors using modified open source code OpenMC(TD)

J. Romero-Barrientos [a, *], F. Molina [a, b, c], J.I. Márquez Damián [d], M. Zambra [a, e], P. Aguilera [a], F. López-Usquiano [a, c, f], S. Parra [a]

[a] Centro de Investigación en Física Nuclear y Espectroscopía de Neutrones CEFNEN, Comisión Chilena de Energía Nuclear, Nueva Bilbao, 12501, Las Condes, Santiago, Chile
[b] Millennium Institute for Subatomic Physics at High Energy Frontier - SAPHIR, Fernández Concha 700, Las Condes, Santiago, Chile
[c] Departamento de Ciencias Físicas, Universidad Andres Bello, Sazié 2212, 837-0136, Santiago, Chile
[d] Spallation Physics Group, European Spallation Source ERIC, P.O. Box 176, 22100, Lund, Sweden
[e] Universidad Diego Portales, Manuel Rodríguez Sur 415, Santiago, Chile
[f] Departamento de Física, Facultad de Ciencias Físicas y Matemáticas, Universidad de Chile, Blanco Encalada, 2008, Santiago, Chile

ARTICLE INFO

Article history:
Received 11 October 2022
Received in revised form
16 January 2023
Accepted 3 February 2023
Available online 8 February 2023

Keywords:
OpenMC
Monte Carlo
Transient Monte Carlo
Open source
Individual precursors

ABSTRACT

In deterministic and Monte Carlo transport codes, β-delayed emission is included using a group structure where all of the precursors are grouped together in 6 groups or families, but given the increase in computational power, nowadays there is no reason to keep this structure. Furthermore, there have been recent efforts to compile and evaluate all the available β-delayed neutron emission data and to measure new and improved data on individual precursors. In order to be able to perform a transient Monte Carlo simulation, data from individual precursors needs to be implemented in a transport code. This work is the first step towards the development of a tool to explore the effect of individual precursors in a fissile system. In concrete, individual precursor data is included by expanding the capabilities of the open source Monte Carlo code OpenMC. In the modified code – named Time Dependent OpenMC or OpenMC(TD)– time dependency related to β-delayed neutron emission was handled by using forced decay of precursors and combing of the particle population. The data for continuous energy neutron cross-sections was taken from JEFF-3.1.1 library. Regarding the data needed to include the individual precursors, cumulative yields were taken from JEFF-3.1.1 and delayed neutron emission probabilities and delayed neutron spectra were taken from ENDF-B/VIII.0. OpenMC(TD) was tested in a monoenergetic system, an energy dependent unmoderated system where the precursors were taken individually or in a group structure, and in a light-water moderated energy dependent system, using 6-groups, 50 and 40 individual precursors. Neutron flux as a function of time was obtained for each of the systems studied. These results show the potential of OpenMC(TD) as a tool to study the impact of individual precursor data on fissile systems, thus motivating further research to simulate more complex fissile systems.

1. Introduction

Two types of neutrons are emitted in a nuclear fission reaction: prompt and delayed neutrons. Prompt neutrons, emitted almost instantaneously (~ 10^{-14} s) after a fission event occurs, have energies of the order of a few MeV. On the other hand, delayed neutrons, are emitted from milliseconds to tens of seconds after the fission event and its energies are of the order of hundreds of keV. This delayed emission is associated to the half-life of the β-decay corresponding to the fission product parent nucleus. Nuclei that are emitters of β-delayed neutrons are called *delayed neutron precursors* or *precursors* [1]. If there is enough fissile material, a neutron can induce fission in other nuclei, thus initiating a fission chain reaction. From this reaction, many delayed neutron precursor isotopes can be produced, for example, for ^{235}U there are about 540 fission products and 270 precursors [2]. Traditionally, all these precursors have been grouped in 6 families or groups. Each of these groups consists of different isotopes and is characterized by a group constant, a group relative yield and a group energy spectrum. This

* Corresponding author.
E-mail address: jaime.romero@cchen.cl (J. Romero-Barrientos).

https://doi.org/10.1016/j.net.2023.02.006

structure was proposed originally by Keepin [1] in 1957, assuming that delayed neutron decay activity can be represented as a sum of exponential decays periods. Even though this grouping is generally used in deterministic or Monte Carlo simulations, it limits the opportunity to study how new and improved nuclear data on individual precursors impacts quantities such as the time evolution of the neutron flux. There has been a renewed interest in the measurement of nuclear decay properties of the most neutron-rich nuclei, such as decay half-lifes, neutron emission probabilities and production yields [3], along with efforts from the International Atomic Energy Agency Coordinated Research Project on a *Reference Database for β-delayed Neutron Emission* [4]. This scenario brings the opportunity to explore how new individual precursor data impacts on simulations of fissile systems. This work presents the methodology and results obtained when explicitly including the time dependence related to the β-delayed neutron emission from individual precursors in a Monte Carlo simulation. This entails two challenges, the first is the inclusion of delayed neutron emission in a Monte Carlo simulation and the second is the addition of data from individual precursor in the simulation. The open source transport Monte Carlo code OpenMC was chosen [5] to include these modifications. The work presented here is a summarized and revised version of the corresponding author's Ph. D thesis [6,7].

2. β-Delayed neutron emission in fissile systems

β-Delayed emission is produced when a fission product (Z, N) decays via a β^- process with a father-daughter atomic mass difference Q_β. If this mass difference Q_β is greater than the neutron separation energy S_n, then excited states in the daughter nucleus $(Z+1, N-1)$ can be populated. This nucleus in turn can decay to the nucleus $(Z+1, N-2)$. Although the neutron is emitted instantaneously, the time scale of this emission is related to the half-life of the β^- decay corresponding to the (Z, N) nucleus. This parent β-decay nucleus (Z, N) is known as *delayed neutron precursor* or *precursor*.

In a nuclear fission chain reaction a large number of delayed neutron precursor isotopes can be produced. In 1957, Keepin measured the periods, relative abundances and yields of delayed neutrons from fission and proposed to group all of these precursors in 6 groups, by assuming that their decay activity could be represented as a linear superposition of exponential decay periods, i.e.,

$$A(t) = \sum_{j=1}^{6} a_j \exp(-\lambda_j t), \tag{1}$$

where $A(t)$ is the measured decay activity, a_j the relative abundance of group j, and λ_j the decay constant of group j. Is important to notice that the measured decay activities, relative abundances, and group decay constants are specific for each fissile target (i.e. ^{235}U or ^{239}Pu) and incident neutron energy (i.e. thermal or fast fission). These groups and its parameters are shown in Table 1 for the case of thermal fission of ^{235}U.

Delayed neutrons play an important role in nuclear reactor applications [8,9]. For instance, in the design of a nuclear reactor, they are related to parameters that characterize its global response from a kinetic point of view such as the effective delayed neutron fraction, the effective neutron generation time, and the reactor period. During the operation of a nuclear reactor, delayed neutron data is used as input to perform the calibration of control rods, and in the case of safety, delayed neutrons are related to transient states produced by changes in reactivity.

The different time scales of prompt and delayed neutrons have consequences when these emissions are included in a Monte Carlo simulation. To further discuss this issue, since delayed neutron precursor decay is a stochastic process, it can be described by

$$p_i(t) = \lambda_i e^{-\lambda_i (t - t_0)}, \tag{2}$$

with $p_i(t)$ being the decay probability density for the i-th precursor at a given time t, λ_i the decay constant for the i-th precursor and t_0 the creation time of the precursor. With this probability, an *analog* Monte Carlo simulation could be performed to describe a fissile system: at a time t_f of the fission event, ν_p prompt neutrons are produced and afterwards, at a time $t = t_f + t_d$, ν_d delayed neutrons are inserted into the simulation. Time t_d is sampled from decay probability Eq. 2, while the energy is sampled from the precursor delayed neutron energy distribution. Though this strategy emulates the events in a nuclear reactor, different timescales associated to prompt and delayed events would result in large variances. As it was mentioned, there is a time delay between the nuclear fission event and the emission of a delayed neutron from the precursor decay. To further illustrate this point, the average lifetime of a prompt neutron in a light water reactor is about 10^{-4} s and the average number of neutrons in a fission chain for a system close to critical is ~ 150 neutrons [10]. This means that the average lifetime of a neutron chain is about 10^{-2} s. On the other hand, a prompt fission chain in a critical reactor will, on average, produce one precursor, which in turn will decay and emit a delayed neutron that will produce a new fission chain in a few seconds. There will be no new neutrons produced during this time, so in an analog Monte Carlo simulation there will be no particles scored, thus obtaining results with large variances. To overcome this problem, the decay of precursors must be simulated in another way.

Related to the β-delayed neutron emission from individual precursors, instead of using the traditional precursor structure, there are 5 quantities needed to characterize individual precursor nuclides: i) fission yield, ii) precursor delayed neutron emission probability, iii) average delayed neutron yield, iv) precursor decay constant, and v) precursor delayed neutron spectrum. Now each of this quantities will be reviewed:

Cumulative fission yield (*CY*)*:* Defined as the number of atoms of a specific nuclei that are produced directly from fissions and via decay of precursors. For instance, *CY* for ^{87}Br is 2.03% in ENDF/B-VIII.0 [2], which means that 203 atoms of ^{87}Br are created per 10,000 fissions.

Precursor delayed neutron emission probability (P_n)*:* Represents the probability of a neutron emission. Following the example, in ENDF/B-VIII.0^{87}Br has a 2.6% probability of decaying to ^{86}Kr, emitting a delayed neutron in the process, so, if 203 atoms of ^{87}Br are produced per 10,000 fissions, and they have a 2.6% probability of decaying to ^{86}Kr, then they will emit 5.3 delayed neutrons per 10,000 fissions.

Average delayed neutron yield (ν_d)*:* Average number of delayed neutrons produced per fission. It can be measured or it can be calculated using the cumulative yield and the precursor delayed neutron emission probability,

Table 1
Six precursor groups and its corresponding decay constants and relative abundances for the thermal fission of^{235}U from Keepin's experiment [1].

Group	λ_j (s^{-1})	a_j
1	0.0124(3)	0.033(3)
2	0.0305(9)	0.219(9)
3	0.111(4)	0.196(22)
4	0.301(12)	0.395(11)
5	1.14(15)	0.115(9)
6	3.01(29)	0.042(8)

$$\nu_d = \sum_i^N CY_i\, P_{n,i}, \tag{3}$$

where N is the number of precursors.

Precursor decay constant (λ)*:* Represents the probability for a precursor to decay per time unit and it is proportional to the number of precursors:

$$\lambda = -\frac{1}{N}\frac{dN}{dt}. \tag{4}$$

Precursor delayed neutron spectrum (χ_d)*:* Characterizes the energy distribution of the delayed neutrons emitted by each precursor. At this moment there are only 34 evaluated experimental spectra, the rest obtained by using QRPA calculations [11]. Due to this fact, in this work the "average energy" of the emitted delayed neutrons was used, so all the precursors are balanced with regard to the β-delayed neutron emission energies. A detailed discussion where β-delayed average neutron energy for the 8-group precursor structure in OpenMC(TD) is compared with the neutron spectrum energy for the JEFF-3.1.1 8-group precursor structure can be found in the corresponding author's PhD thesis [6,7].

3. OpenMC Monte Carlo code

The Monte Carlo code OpenMC [5] is a relatively new, open-source code for particle transport developed originally at the Massachusetts Institute of Technology in 2013. It is currently being developed and maintained by a community of researchers across multiple institutions. This code is capable of simulating neutron transport in fixed source, k-eigenvalue, and subcritical multiplication problems. The code supports both continuous-energy and multigroup cross sections. OpenMC estimates physical quantities, such as neutron flux, through *tallies*; *filters* are used to specify a region of the phase space, for example, scoring neutron flux for a given cell position. The continuous-energy nuclear cross section data follows the HDF5 format [12] and is generated from ACE files produced by NJOY [13]. Since this code is open source, its license allows to modify the source code to develop and add new capabilities. An example of this last point is the many number of publications associated to the code, covering topics and developments such as benchmarking [14], coupling and multi-physics [15], geometry and visualization [16], multigroup cross section generation [17], doppler broadening [18], nuclear data [19], parallelism [20], depletion [21] and sensitivity analysis [22].

4. Methodology

The methodology used to include the β-delayed neutron emission from individual precursors in a Monte Carlo simulation is presented in this section. First, it is shown how time dependence in Monte Carlo was included. After that, the implementation of individual precursors is discussed, and finally, strategies related to overcome the large variances associated with the different time scales between prompt and delayed neutrons are detailed. These additions were part of the work developed during the corresponding author's PhD thesis [6,7], using the version of OpenMC 0.10, written in Fortran. Current version of OpenMC is 0.13.0, written in C++.

4.1. Time dependence in Monte Carlo

Given that time is not explicitly present in a Monte Carlo simulation, there are some issues that needs to be addressed before considering the time delay of the delayed neutrons emitted by the precursors. The first is to account for the time evolution of neutrons, by adding a time label t to the particles, which would serve as a clock, with a value that is updated using the kinetic energy and the distance traveled by the neutron between events. The initial value for this label is set to zero ($t = 0$) at the beginning of the simulation and is updated as the particle is transported through the simulation. To score measured quantities in time, this is, to score the time evolution of observables in the simulation, a *time filter* was developed to add the capability to monitor the time evolution of any of the tallies already present in the code. These two features were presented and used to calculate two kinetic parameters: the effective delayed neutron fraction β_{eff} and neutron generation time Λ in a previous article [23]. The last feature needed to perform transient Monte Carlo simulations is the division of the total simulation time in discrete time intervals. There are two reasons behind this: the first one is related to variance reduction and population control methods implemented, which need a *time grid* to be applied. The second reason is that in a transient simulation changes to the geometry or reactivity can occur, and these changes can be introduced at the end of a time interval.

4.2. Emission from individual precursors

At the time of writing this work there are no published Monte Carlo codes for neutron transport in fissile systems that include delayed neutron emission from individual precursors. Usually, if a delayed neutron is sampled, then the next step is to choose which precursor group will be sampled. Here, the relative yield for the traditional 6- or 8-group structure is utilized. If the j-th group is selected, then the delayed time associated with the delayed emission is sampled using the j-th group decay constant and Eq. (2). Finally, the delayed neutron energy is chosen from the j-th delayed neutron energy group spectrum, and the delayed neutron is inserted directly into the simulation. In this work, if a delayed fission is sampled, instead of directly inserting a delayed neutron in the simulation, a precursor is produced. After this, which precursor will decay must be chosen. To do this, the precursor importance or relative abundance of the individual precursor i-th, I_i, defined as [24].

$$I_i \equiv \frac{CY_i\, P_{n,i}}{\nu_d}, \tag{5}$$

is used, with CY_i the cumulative fission yield, $P_{n,i}$ the precursor delayed neutron emission probability, and ν_d the average delayed neutron yield. The cumulative yield is used because given that the initial transient source is constructed from a converged source obtained from an eigenvalue calculation, an equilibrium state is assumed. With the precursor chosen, the delayed time associated to the emission is sampled using the precursor decay constant along with Eq. 2. Lastly, the delayed neutron energy is the average energy from the corresponding precursor delayed energy spectrum.

As for the number of precursors included in the simulations, the precursor importance shows the fraction of the total delayed neutron yield that the precursor represents. To illustrate this point, when using the *CY* from JEFF-3.1.1 [25] library and P_n from ENDF/B-VIII.0, the average neutron yield obtained is 1.57×10^{-2}. Then, using Eq. (5), the importance of ^{137}I is 0.1626, which means that delayed neutrons emitted from the decay of this precursor account for 16.26% of the total β-delayed neutron emission. Although there are data for 269 precursors, in this the 50 most important precursors will be included, since they account for 99.16% of the total delayed neutron yield. The list of the 50 individual precursors used can be

found in Appendix E of Ref. [6,7]. The delayed neutron yield was renormalized to the emission from the 50 selected precursors. Table 2 summarizes the differences when comparing between the simulation of β-delayed neutron emission using the traditional group structure versus using individual precursors.

4.3. Delayed neutron precursors

4.3.1. The precursor particle

To include the precursor decay in the simulation, a new particle is defined in the code, the *precursor particle*. All individual precursors, or precursor groups, are combined into a single precursor particle [10]. The decay probability for this particle is

$$p_{combined}(t) = \sum_i \Gamma_i \lambda_i e^{-\lambda_i (t-t_0)}, \tag{6}$$

here t_0 is the time when the precursor particle was created, and Γ_i is a factor that depends on whether individual precursors or precursor groups are being considered:

$$\Gamma_i = \begin{cases} \frac{\beta_i}{\beta}, & \text{for precursor groups.} \\ I_i, & \text{for individual precursors.} \end{cases} \tag{7}$$

With β_i the delayed fraction for the i-th precursor group and $\sum_i \beta_i = \beta$, and β is the total delayed neutron fraction. If individual precursors are being considered, then I_i is the precursor importance for the i-th individual precursor.

4.3.2. Forced decay

An analog simulation of delayed neutrons produced from precursor decay would lead to significant variance in results obtained, thus another way to simulate the delayed emission must be used. Given that this variance is originated by the fact that there are too few fission chains per unit time caused by decays from delayed neutrons, one strategy would be to modify the precursor decay probability, forcing the decay of all the precursors in each interval, producing more delayed neutrons. This technique is called "forced decay" [26] and it requires biasing the sampling of delayed neutrons, while preserving the Monte Carlo fair game by altering the statistical weight of the emitted delayed neutrons. The simplest choice for this biased decay probability is a uniform decay probability, forcing the decay of all the precursors in each one of the time intervals in which the simulation is divided, this is

$$\overline{p}(t) = \frac{1}{t_{j+1} - t_j} = \frac{1}{\Delta t}, \tag{8}$$

where t is the time when forced decay happens and Δt is the length of the time interval. The statistical weight of the produced delayed neutrons must be adjusted to

$$w_d(t) = \frac{p(t)}{\overline{p}(t)} = w_c \, \Delta t \sum_i \Gamma_i \lambda_i e^{-\lambda_i (t-t_0)} \quad \text{with} \quad t_j < t < t_{j+1}, \tag{9}$$

where w_c corresponds to the statistical weight of the precursor. The delayed neutron produced will be transported and can cause new fissions. Once the delayed neutron of weight $w_d(t)$ was created, the precursor is not eliminated from the simulation. Instead, it is added to a precursor bank with weight

$$w_p(t) = w_c \sum_i \Gamma_i e^{-\lambda_i (t_{i+1} - t_i)}. \tag{10}$$

This precursor will undergo forced decay, producing more delayed neutrons. It is important to notice that precursors are not being transported and only interact with the simulation through the delayed neutrons that emits.

4.4. Initial transient source

To start a transient Monte Carlo simulation, an initial transient source distribution is constructed using a previously converged source distribution obtained from an eigenvalue calculation, with effective multiplication source $k_{eff} \sim 1$. To asses the convergence of the source distribution in the criticality calculation, OpenMC has the capability to define a suitable spatial mesh to monitor the Shannon entropy. This initial transient source can be created by two methods. The first one is by transforming the neutron source obtained from a criticality calculation into a mixed source, comprised of neutrons and precursors. The second method requires the sampling of the initial neutrons and precursors using appropriate tallies after the eigenvalue calculation. For the case of a 1-group monoenergetic system, the first method is an acceptable choice. In this case, to determine the fractions of neutrons at a given position $\mathbf{r}$ the following relation is used:

$$\frac{n_0(\mathbf{r})}{n_0(\mathbf{r}) + C_0(\mathbf{r})} = \frac{1}{1 + \frac{\beta}{\lambda} \nu \Sigma_f}, \tag{11}$$

where $n_0(\mathbf{r})$ is the initial number of neutrons, $C_0(\mathbf{r})$ is the initial number of precursors, β is the delayed neutron fraction, λ is the precursor decay constant, ν is the delayed neutron yield, v is the neutron speed, and Σ_f is the fission cross section. This relation is valid only when considering neutrons of constant energy. For the monoenergetic system studied in this work, it is obtained that for every neutron there are about 10^4 precursors, and that the fraction of prompt neutrons in steady state is of the order of 0.08%.

When using the second method [10] the energy dependent initial transient source is sampled from an eigenvalue calculation, with the number of neutrons calculated using the estimator

$$n_0(\mathbf{r}, E) = \int_{4\pi} \frac{\psi_0(\mathbf{r}, \mathbf{\Omega}, E)}{\nu(E)} d\mathbf{\Omega}, \tag{12}$$

meanwhile the initial number of precursors is obtained using

$$C_{i,0}(\mathbf{r}) = \int_{4\pi} \int_0^\infty \frac{\beta_i(\mathbf{r}, E) \nu(\mathbf{r}, E) \Sigma_f(\mathbf{r}, E)}{\lambda_i} \psi_0(\mathbf{r}, \mathbf{\Omega}, E) dE d\mathbf{\Omega}, \tag{13}$$

where ψ_0 is the neutron flux, sampled by an already existing flux

Table 2
Differences when using the precursor group structure or the individual precursors.

Quantity	N-group structure	This work
Relative abundance	β_i/β with $1 < i < 6$ or 8	$(CY_i \, P_{n,i})/\nu_d$ with $1 < i < 50$
Decay constants	Precursors in 6- or 8- groups	50 individual precursors
Energy spectra	Precursors in 6- or 8- groups	50 individual precursors

tally in OpenMC. There should be mentioned that the probability distribution for precursors created in a fission event is different than the one for precursors created from a steady state situation, because precursors have undergone a portion of its decay before $t = 0$. Different precursors with different decay constants result in a steady state fraction of the total number of precursors, P_i, given by

$$P_i = \begin{cases} \frac{\lambda^b}{\lambda_i}\frac{\beta_i}{\beta}, & \text{for precursor group} \\ \frac{\lambda^b}{\lambda_i} I_i, & \text{for individual precursor,} \end{cases} \tag{14}$$

where λ^b is the inversely weighted decay constant defined as

$$\lambda^b = \begin{cases} \frac{\beta}{\sum_i \frac{\beta_i}{\lambda_i}}, & \text{for precursor group} \\ \frac{1}{\sum_i \frac{I_i}{\lambda_i}}, & \text{for individual precursor,} \end{cases} \tag{15}$$

This difference in the probability distributions is implemented in the code according to the creation time of the precursor.

4.5. Population control

In the *forced decay* method precursors are always kept in the simulation after they decay into delayed neutrons. This means that the population of precursors continuously increases, so it must be controlled. The population control method implemented in the OpenMC code in this work is the *combing method* [27], originally developed for stationary Monte Carlo simulations. The idea behind this method is to preserve the total statistical weight, while maintaining a fixed number of particles where all the statistical weights are set to be the average weight. Keeping constant the number of particles contributes to reduce computing time by maintaining the population size approximately constant, while, by setting the weight of each particle to be the same, statistical fluctuations are reduced [28,29]. If the system is super-critical, combing prevents the unchecked growth of the population, while if the system is sub-critical, it keeps the simulation running by preventing the population from dying. If the system is critical, combing prevents the divergence of the population due to fluctuations of fission chains [30].

In this method, if there are K particles at the end of a time interval, with total statistical weight W, and the objective is to comb them to M particles, then these K particles will be combed into M using a comb with M teeth. Each combed particle is assigned a statistical weight $w' = \frac{W}{M}$. Fig. 1 shows an example situation with $K = 4$ and $M = 3$. Fig. 2 shows an example where $K = 5$ and $M = 10$. In this work both the neutron and precursor populations are combed separately.

5. Results and discussion

The time dependence in neutron transport, including β-delayed neutron emission from individual precursors, was added to the original OpenMC code. Then the modified version of the code, called Time-Dependent OpenMC or OpenMC(TD), was tested in a system consisting of a rectangular box of 10 cm × 12 cm × 20 cm, surrounded by vacuum. For the first test, the system was made monoenergetic and 1-group precursor was used. Here, three cases were studied: subcritical, critical and a case where reactivity was inserted into the system. For the second test, the system was made energy dependent, studying a fast unmoderated ^{235}U system, where two configurations were studied and discussed: subcritical and supercritical. For the final tests, the fast unmoderated ^{235}U system was surrounded with light-water, thus studying a moderated energy dependent system, and different precursor structures were used. Computer simulations were run at CSICCIAN (Spanish acronym for Simulation and Calculation Center for Nuclear Sciences and Applications) clusters from the Chilean Nuclear Energy Commission.

5.1. Monoenergetic fissile system with 1-group precursor structure

The division of the simulation in discrete time intervals, scoring of time dependent quantities, precursor forced decay and population control, were tested in a monoenergetic system, characterized by the parameters shown in Table 3. These tests had the objective of laying the groundwork to study the delayed neutron emission from individual precurors for transient simulations with OpenMC(TD). Before performing transient simulations with OpenMC(TD), a non-transient standard criticality calculation was done using OpenMC with 10^6 neutrons, 3000 batches[1] and 200 skipped cycles, to obtain the effective multiplication factor, which was $k_{eff} = 1.00010(3)$. After this calculation, the initial transient source was created as described in Sec. 4.4, with 10^5 neutrons and 9×10^5 precursors. In this section the inputs were the macroscopic cross section Σ_a, which were modified accordingly to produce reactivity changes in the monoenergetic fissile system. Output values (i.e., observables) were the effective multiplication factor k_{eff}, and the time evolution of the neutron population $n(t)$, which were compared with point kinetics calculations. Additional criticality calculations performed in Section 5.1.1 and Section 5.1.2 were run with 10^6 neutrons, 3000 batches and 200 skipped cycles.

5.1.1. Subcritical configuration

The monoenergetic system was made subcritical by increasing the absorption cross section from $\Sigma_a = 0.5882$ cm^{-1} to $\Sigma_a = 0.5952$ cm^{-1}, while keeping the total cross section Σ_t constant, thus obtaining an effective multiplication factor $k_{eff} = 0.98821(3)$. This increase in the absorption cross section Σ_a is analog to reducing the fissile material density of the system. This simulation was executed with 60 batches, and the total simulation time was 50 s, divided in 500 time intervals of 100 ms. At the end of each time interval population control was applied. Results obtained by using OpenMC(TD) are shown in blue in Fig. 3, while the point kinetic solution for the time evolution of the neutron population is shown in red (see Eq. (16)). Explicitly, the point kinetic solution was

$$n(t) = n_0\left[\frac{\rho}{\rho-\beta}\exp\left(\frac{\rho-\beta}{\Lambda}t\right) - \frac{\beta}{\rho-\beta}\exp\left(-\frac{\lambda\rho}{\rho-\beta}t\right)\right], \tag{16}$$

where $n(t)$ is the neutron population at time t, n_0 is the neutron population at $t = 0$, ρ is the system reactivity, β is the delayed neutron fraction, Λ is the neutron generation time and λ is the decay constant. From Fig. 3 can be seen that the neutron population as a function of time calculated using transient Monte Carlo code OpenMC(TD) and point kinetics solution are equivalent. Quantitatively, from Fig. 3 the reactivity ρ can be obtained as a fitted parameter from the point kinetics equation (see Eq. (16)). This

[1] In a Monte Carlo simulation, a batch is a single realization of a tally random variable. In the simulation both the number of batches as well as the number of particles per batch must be specified.

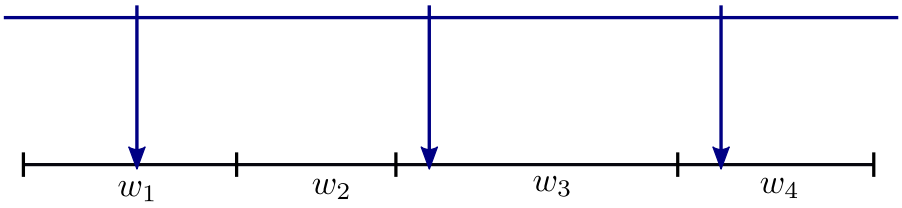

Fig. 1. Diagram explaining the application of the combing method for 4 particles of total weight W combed into $M = 3$. The particles kept by the comb are particle 1, particle 3 and particle 4, each with weight $W/3$, preserving the total weight W.

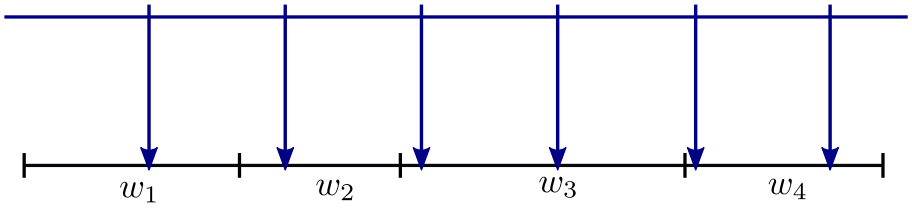

Fig. 2. Diagram explaining the application of the combing method for 4 particles of total weight W combed into $M = 6$. The particles kept by the comb are particle 1, particle 2, particle 3 (×2), and particle 4 (×2), each with weight $W/6$, preserving the total weight W.

Table 3
Parameters and material cross sections of the monoenergetic system.

Parameter	β_{eff}	λ (s^{-1})	ν	Σ_t (cm^{-1})	Σ_f (cm^{-1})	Σ_a (cm^{-1})	Σ_s (cm^{-1})	ν ($cm\ s^{-1}$)
Value	0.00685	0.0784	2.5	1.0	0.25	0.5882	0.4118	2.2×10^4

fitted reactivity $\rho_{fit} = -0.01191(1)$ was compared to the reactivity obtained from the criticality calculation $\rho = (k_{eff} - 1)/k_{eff} = -0.01193(3)$.

5.1.2. Slightly supercritical configuration

Afterwards, the code was used to study the transient behavior in a slightly supercritical configuration, with $k_{eff} = 1.00010(3)$. Total simulation time was 25 s, divided in 250 time intervals of 100 ms each, and 4 batches were used. The combing method was applied at the end of each time interval. Results obtained by using OpenMC(TD) are shown in blue in Fig. 4, where it can be seen that the neutron population as a function of time calculated using transient Monte Carlo simulation with OpenMC(TD) and point kinetics solution (see Eq. (16)) are equivalent. Neutron population remains practically constant, as it is expected for a system close to criticality. Quantitatively, from Fig. 4 the reactivity ρ can be obtained as a fitted parameter from Eq. (16). This fitted reactivity $\rho_{fit} = 0.00014(1)$ was compared to the reactivity obtained from the criticality calculation $\rho = (k_{eff} - 1)/k_{eff} = 0.00010(3)$.

5.1.3. Reactivity insertion

The last case studied for the monoenergetic system was a reactivity insertion. The system started slightly supercritical at $t = 0$, then at $t = 10$ s, Σ_a was reduced from $\Sigma_a = 0.5882\ cm^{-1}$ to $\Sigma_a = 0.5870\ cm^{-1}$, thus increasing the system reactivity by 211 pcm, making the configuration supercritical. At $t = 40$ s the system is brought back to $\Sigma_a = 0.5882\ cm^{-1}$. The final state corresponds to a slightly supercritical configuration. Total simulation time was 50 s, divided in 5000 time intervals of 10 ms each, and 25 batches were used. The combing method was applied at the end of each time interval. Results obtained by using OpenMC(TD) are shown in blue in Fig. 5, where it can be seen that the neutron population as a function of time calculated using transient Monte Carlo simulation with OpenMC(TD) and point kinetics solution from Eq. (16) are equivalent.

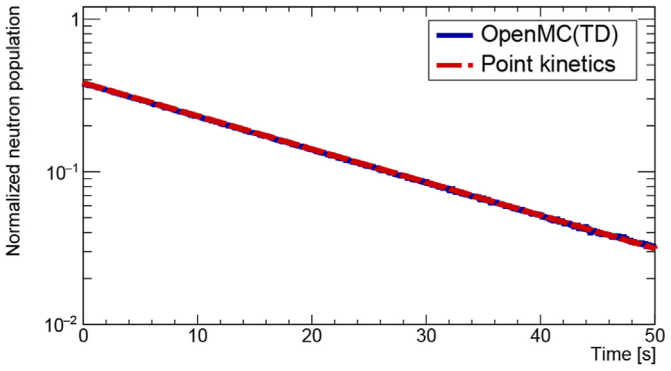

Fig. 3. (Color online). Neutron population as a function of time for a monoenergetic system in a subcritical configuration ($k_{eff} = 0.98821(3)$ obtained using OpenMC(TD). Result is compared to the analytical solution obtained from point kinetics equations. (For interpretation of the references to color in this figure legend, the reader is referred to the Web version of this article.)

5.2. Energy-dependent ^{235}U system

After OpenMC(TD) was tested in the monoenergetic system described in the previous section, the next study was testing the code in a system with continuous, energy-dependent cross sections. The objective was to test the capabilities of the code in a model with increased complexity, while keeping it simple enough to compare its results to the ones from point kinetics model. To achieve this, the material of the box from the preceding section was made of pure ^{235}U, using continuous cross sections from JEFF-3.1.1

[25] nuclear data library and this box was surrounded by vacuum. Before performing transient simulations with OpenMC(TD), a non-transient standard criticality calculation was done using OpenMC with 10^6 neutrons, 5000 batches and 300 skipped cycles, to obtain the effective multiplication factor, which was $k_{eff} = 1.00015(3)$. After this calculation, the initial transient source was created, with 10^5 neutrons and 9×10^5 precursors. This transient source was used in subcritical and supercritical configurations in order to start the transient simulation. In this section the input was the density of fissile material, represented by n_{U235}, because to simulate a reactivity insertion, the density of fissile material was changed, keeping the dimensions of the box constant. Output values (i.e., observables) were the effective multiplication factor k_{eff}, and the time evolution of the neutron flux $\phi(t)$. To calculate Λ and β_{eff}, a simulation in MCNP was performed, because this code can estimate these parameters using the weighted adjoint flux. These two quantities were the compared with the fitted parameters from point kinetics solutions. Continuous energy cross sections used for MCNP simulations were from JEFF-3.1.1 [25] nuclear data library. Additional criticality calculations performed in Section 5.2.1 and Section 5.2.2 were run with 10^6 neutrons, 3000 batches and 200 skipped cycles. In this section, six cases with different precursor structures were studied for a subcritical and for a supercritical system. A summary of these studies is shown in Table 4, where the notation for the delayed neutron energy is as follows: $\chi_1(E)$ corresponds to energy sampled from the first group spectrum from JEFF-3.1.1, E_{1g} refers to the average energy from the first group from JEFF-3.1.1, E_{6g} uses the average energy from 6 precursor group structure from ENDF-B/VIII.0, $\chi(E)$ corresponds to the energy sampled from spectra, and E_i refers to average energy for each group or individual precursor. In this article only one case is shown, but all cases are described in further detail in the corresponding author's PhD thesis [6,7], where in summary, discrepancies were found in the value obtained for the effective delayed neutron fraction using JEFF-3.1.1 and ENDF-B/VIII.0 nuclear libraries, which shows the relevance of appropriate nuclear data for individual precursors.

5.2.1. Subcritical configuration

The system was made subcritical by decreasing the fissile material density from $n_{U235} = 4.496 \times 10^{-2}$ (atoms/b cm) to $n_{U235} = 4.4362 \times 10^{-2}$ (atoms/b cm), while keeping the box dimensions constant, thus making the effective multiplication of the system $k_{eff} = 0.98956(3)$. Total simulation time was 0.1 ms, divided in 1000 time intervals of 100 ns each, and 22 batches were simulated. The combing method was applied at the end of each time interval to control the particle population. Results obtained by using OpenMC(TD), for the case when the average energy from JEFF-3.1.1 was used, are shown in blue in Fig. 6, while the fit obtained by adjusting the results to the point kinetics solution are shown in red. From Fig. 6 the prompt drop can be observed for the first 5 μs, and then for $t > 5\mu$s the neutron flux decay stabilizes. From a quantitative point of view, fitted effective neutron generation time obtained was $\Lambda_{fitted} = 5.45(1)$ ns. MCNP obtained value was $\Lambda_{MCNP} = 5.74(1)$ ns, giving a $\sim 5.1\%$ difference between both quantities. The fitted effective delayed neutron fraction obtained was $\beta_{eff}^{(fitted)} = 0.00666(1)$. MCNP obtained value was $\beta_{eff}^{(MCNP)} = 0.00644(6)$, giving a $\sim 2.8\%$ difference between both quantities.

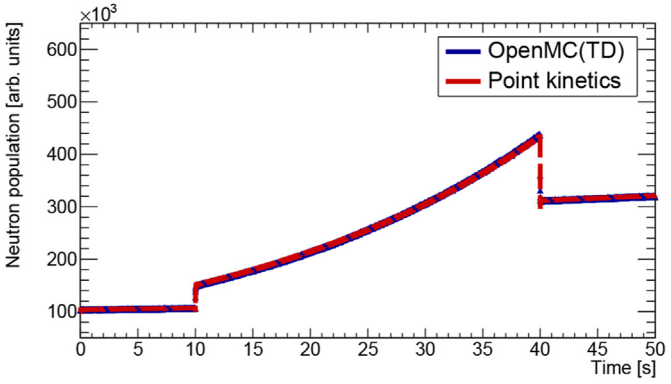

Fig. 5. (Color online). Neutron population as a function of time for a monoenergetic system obtained using OpenMC(TD). The system is initially in a slightly supercritical configuration, then, at $t = 10$ s a reactivity of 211 pcm is inserted. After 30 s the system is brought back to its initial slightly supercritical configuration. (For interpretation of the references to color in this figure legend, the reader is referred to the Web version of this article.)

5.2.2. Supercritical configuration

The system was made supercritical by increasing the fissile material density from $n_{U235} = 4.496 \times 10^{-2}$ (atoms/b cm) to $n_{U235} = 4.511 \times 10^{-2}$ (atoms/b cm), while keeping the box

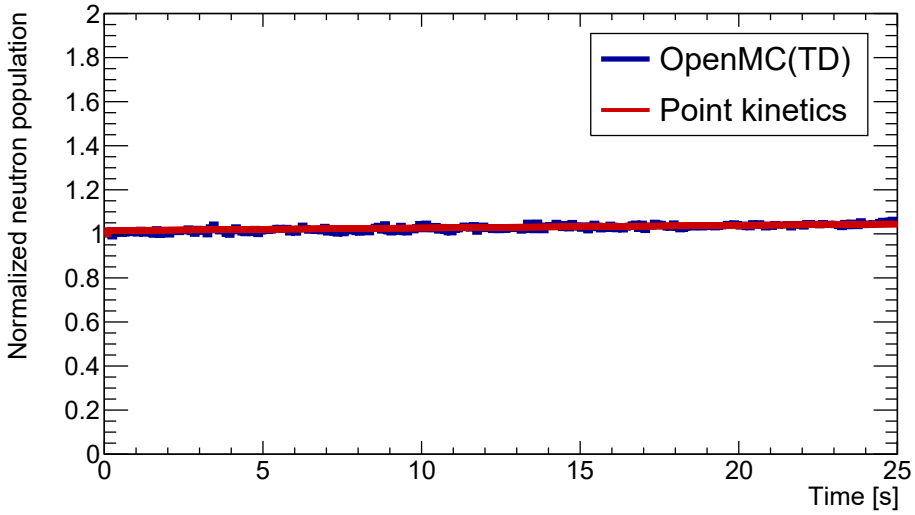

Fig. 4. (Color online). Time evolution of the neutron population for a monoenergetic system in a critical configuration ($k_{eff} = 1.00010(3)$ obtained using OpenMC(TD)). Result is compared to the analytical solution from the point kinetics equations. (For interpretation of the references to color in this figure legend, the reader is referred to the Web version of this article.)

dimensions constant, thus making the effective multiplication of the system $k_{eff} = 1.00271(3)$. Total simulation time was 0.1 ms, divided in 1000 time intervals of 100 ns each, and 22 batches were simulated. The combing method was applied at the end of each time interval to control the particle population. Results obtained by using OpenMC(TD), for the case when the average energy from JEFF-3.1.1 was used, are shown in blue in Fig. 7, while the fit obtained by adjusting the results to the point kinetics solution are shown in red. From Fig. 7 the prompt jump can be observed for the first 1 μs, and then for $t > 1\mu s$ the neutron flux growth stabilizes. From a quantitative point of view, fitted effective neutron generation time obtained was $\Lambda_{fitted} = 5.45(1)$ ns. MCNP obtained value was $\Lambda_{MCNP} = 6.00(1)$ ns, giving a difference of 9.2% between both quantities. The fitted effective delayed neutron fraction obtained was $\beta_{eff}^{(fitted)} = 0.00666(1)$. MCNP obtained value was $\beta_{eff}^{(MCNP)} = 0.00651(6)$, giving a difference of 2.3% between both quantities.

Regarding the differences between fitted and calculated mean generation times, it can be mentioned that MCNP calculates Λ using the adjoint weighted flux, while in this work Λ is fitted to point kinetics equation. Although this approximation might be reasonable given the simple geometry under study, some differences could still be expected to arise. To explore if these differences are related to how far from criticality the system is, mean generation times were calculated for the slightly supercritical system of Section 5.3. MCNP obtained value was $\Lambda_{MCNP} = 3.43(2)\mu s$, while fitted generation time was $\Lambda_{fitted} = 3.52(3)\mu s$, giving a difference of 2.9%, similar to the differences found for the subcritical and critical system. This suggests that these differences might not be related to the criticality state of the system, but instead could be related to the point kinetic assumption made to calculate Λ as a fitted parameter. To further explore this topic, additional research would be needed, which is not directly related to the purpose of this work.

5.3. Light-water moderated energy dependent system with individual precursor structure

The system studied in the preceding section was thermalized by surrounding the ^{235}U box with light-water. β-delayed neutron emission was simulated by individual precursors and results obtained were compared when emission is from 6-group precursor structure. The objective was to increase the complexity of the system and to study the time evolution of the neutron flux when using different precursor structures. Specifically, comparisons where made using the 6-group structure and 50 individual precursors, such as effective multiplication system k_{eff}, and neutron flux as a function of time in a transient simulation. As a final study the 10 most important precursors were removed from the list of the 50 individual precursors used previously, thus keeping 40 individual precursors. The objective of this test was to study the effect of the removal of these precursors on the time evolution of the neutron flux. The configuration was surrounded by a 4.29 cm-thickness light-water moderator and made slightly supercritical by setting the ^{235}U density to $n_{U235} = 3.2671 \times 10^{-2}$ (atoms/b cm).

Table 4
Studies performed in the corresponding author PhD thesis [6,7] with different precursor structures and nuclear databases for the^{235}U system.

Case	Precursor structure	Delayed neutron energy	Library
1	1-group	$\chi_1(E)$	JEFF-3.1.1
2	1-group	E_{1g}	JEFF-3.1.1
3	1-group	E_{6g}	ENDF-B/VIII.0
4	8-group	$\chi(E)$	JEFF-3.1.1
5	6-group	E_i	ENDF-B/VIII.0
6	50 individual	E_i	ENDF-B/VIII.0

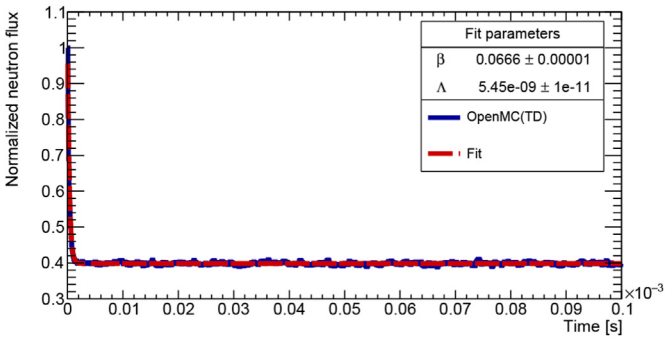

Fig. 6. (Color online). Neutron flux as a function of time in the studied subcritical configuration for Case 1. Initial transient source is prepared in a critical state and at the beginning of the transient Monte Carlo simulation using OpenMC(TD), the system is made subcritical by decreasing n_{U235}. Time evolution of the neutron flux scored by OpenMC(TD) is shown in blue, while the fit obtained is shown in red. Between $0 < t < 5$ μs the prompt drop can be observed, and then the decay of the neutron population slows. (For interpretation of the references to color in this figure legend, the reader is referred to the Web version of this article.)

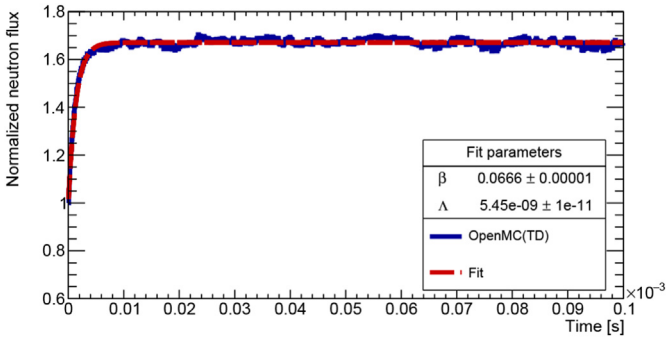

Fig. 7. (Color online). Neutron flux as a function of time in the studied supercritical configuration for Case 1. Initial transient source is prepared in a critical state and at the beginning of the transient Monte Carlo simulation using OpenMC(TD) the configuration is made supercritical by increasing n_{U235}. Time evolution of the neutron flux scored with OpenMC(TD) is shown in blue, while the fit obtained is shown in red. Between $0 < t < 1$ μs the prompt jump can be observed, an then the neutron population growth slows. (For interpretation of the references to color in this figure legend, the reader is referred to the Web version of this article.)

Table 5
Effective multiplication factors obtained for the 4.29 cm thickness water thermalized ^{235}U cube. Results are shown for 6-group structure and 50 individual precursors.

	6-Groups	50 precursors	Difference
k_{eff}	1.00025(3)	1.00032(3)	7(4)

Continuous energy cross section used were from JEFF-3.1.1. The dimensions of the box were not changed. Prior to transient simulations, a non-transient standard criticality calculation was run with 10^6 neutrons, 5000 batches and 300 skipped cycles using OpenMC, obtaining an effective multiplication $k_{eff} = 1.00025(1)$. In this section the code input were the density of fissile material, denoted as n_{U235}, the delayed neutron energy and the number of precursors used (50 or 40). Reactivity was inserted by changing the density of the fissile material. Output values (observables) were the effective multiplication factor k_{eff} and the time evolution of the neutron flux $\phi(t)$. Given that this is not a 1-group precursor problem, there are not analytical solutions to the point kinetics

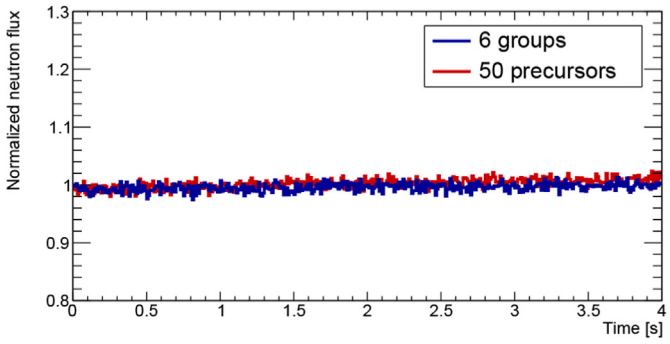

Fig. 8. (Color online). Neutron flux as a function of time in a water moderated box made of pure ^{235}U, simulated with OpenMC(TD). Results for 6 groups are shown in blue, and results for 50 individual precursors are shown in red. Both results show a slightly supercritical system, where neutron flux increases slowly in time, consistent with the k_{eff} of a near critical configuration. (For interpretation of the references to color in this figure legend, the reader is referred to the Web version of this article.)

Table 6
Results obtained for the reactivity of the water moderated energy dependent simulated system in a critical configuration using 6-group and 50 individual precursor structure. Uncertainties for ρ_{fit} were obtained from fit.

	6-Group structure	50 individual structure
ρ [pcm].	25(3)	32(3)
ρ_{fit} [pcm].	17(2)	35(2)

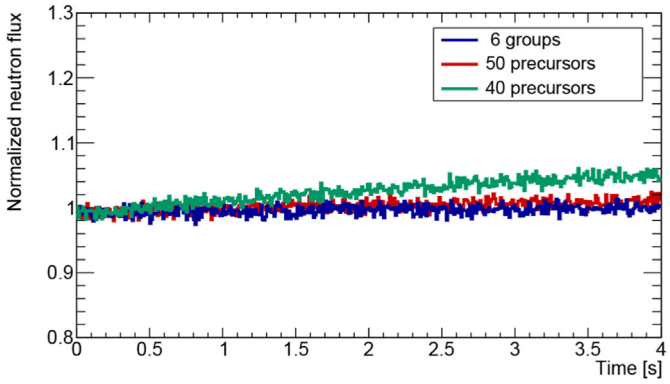

Fig. 9. (Color online). Neutron flux as a function of time in a water moderated box made of pure ^{235}U, simulated with OpenMC(TD). Result when using 6 groups are shown in blue. Results obtained when 50 individual precursors are used are shown in red, while results obtained when using 40 precursors are shown in green. Time evolution of the neutron flux calculated using 40 precursors clearly diverges from the previous results, showing a faster growth of the neutron flux. (For interpretation of the references to color in this figure legend, the reader is referred to the Web version of this article.)

equations, but resorting the point kinetics approximation, a good estimate to the asymptotic decay constant for the neutron flux [1] can be found using the equation

$$\alpha_D = \frac{\bar{\lambda}\rho}{\beta_{eff} - \rho}, \tag{17}$$

where α_D is the asymptotic decay constant, $\bar{\lambda}$ is the average β-weighted decay constant,[2] β_{eff} is the effective delayed neutron fraction and ρ is the reactivity of the system. With respect to the

[2] The average β-weighted decay constant is given by $\bar{\lambda} = \sum \frac{\beta_i}{\beta} \lambda_i$

Table 7
Reactivity of the water moderated energy dependent simulated system in a critical configuration using 6-group, 50 individual and 40 individual precursor structures.

	6-Group structure	50 individual structure	40 individual Structure
ρ_{fit} [pcm].	17(2)	35(2)	111(2)

choice of the delayed neutron fraction, the average delayed neutron yield obtained when using data from JEFF-3.1.1 is $\nu_d = 1.48 \times 10^{-2}$, while the value obtained when using ENDF/B-VIII.0 is $\nu_d = 1.90 \times 10^{-2}$. Taking the average neutron yield as $\nu = 2.4355$ [31], then the delayed neutron fraction, $\beta = \nu_d/\nu$, ranges from $\beta = 607$ pcm to $\beta = 780$ pcm. Considering this, the value for the delayed neutron fraction was chosen to be $\beta_{eff} = 700$ pcm. The decay constant was $\bar{\lambda} = 0.0784\ s^{-1}$. In this study, the reactivity of the system was obtained as a fitted parameter, and then compared to the reactivity obtained from the initial non-transient criticality calculation, $\rho = (k_{eff} - 1)/k_{eff}$.

5.3.1. Criticality calculation using individual precursors

Since before every transient simulation with OpenMC(TD), a non-transient, steady state criticality calculation with OpenMC must be performed to asses the reactivity of the system and to create the initial transient source, and given that during the writing of this article there are no codes that are able to perform a criticality calculation using individual precursors as the source of β-delayed neutron emission, in this work criticality calculations using individual precursors instead of the group structure was also implemented in OpenMC(TD). A slightly supercritical system was obtained when the ^{235}U density was $n_{U235} = 3.2671 \times 10^{-2}$ (atoms/b cm) obtaining $k_{eff} = 1.00025(3)$ for the 6-group structure and $k_{eff} = 1.00032(3)$ for the 50-individual precursor structure. These criticality calculations were run with 10^6 neutrons, 2050 batches and 50 skipped cycles. Results obtained using the 6-group structure and 50 individual precursors are shown in Table 5. The effective multiplication factor obtained for this system shows that this is a slightly supercritical configuration and both results are in good agreement with each other, with a difference of 7 pcm between them.

5.3.2. Slightly supercritical configuration with 50 individual precursor structure

OpenMC(TD) was used to study the behavior of the slightly supercritical configuration, comparing the time evolution of the neutron flux obtained when 6-group and 50 individual precursor structures were used. For both simulations the total simulation time was 4 s, divided in 400 time intervals of 10 ms each, and 2 batches were used. The combing method was applied at the end of each time interval. Wall-clock time for the 6-group precursor simulation was about 260 h, while for the 50 individual precursor simulation was about 411 h. In Fig. 8, results obtained by using OpenMC(TD) are shown in blue for the 6-group structure and in red for 50 individual precursor structure. From Fig. 8 it can be seen that both results show a slightly supercritical system, with a slow increase of the neutron flux. This is consistent with the close-to-critical effective multiplication factor previously obtained.

Quantitatively, the reactivity ρ can be obtained as a fitted parameter of $\phi(t) \sim e^{-\alpha_D t}$ for both 6-group and 50 individual precursor structure. These fitted reactivity values, $\rho_{fit}^{(6)} = 0.00017(2)$ and $\rho_{fit}^{(50)} = 0.00036(2)$, were compared to the reactivity obtained from OpenMC(TD) criticality calculation,

$\rho^{(6)} = (k_{eff}^{(6)} - 1)/k_{eff}^{(6)} = 0.00025(3)$ and $\rho^{(50)} = (k_{eff}^{(50)} - 1)/\ k_{eff}^{(50)} = 0.00032(3)$. Table 6 shows a summary of results obtained.

5.3.3. Slightly supercritical configuration without the 10 most important precursors

Finally, OpenMC(TD) was used to study the same slightly supercritical configuration, but in this case the 10 precursors with the largest importances I_i were removed from the previous list of 50 individual precursors, to study the impact of this removal on the neutron flux as a function of time. This implies that a 40 individual precursor structure was used in this calculation. Total simulation time was 4 s, divided in 400 time intervals of 10 ms each, and 2 batches were used. The combing method was applied at the end of each interval. Wall-clock time for this simulation was about 320 h.

In Fig. 9 results obtained by OpenMC(TD) are shown in blue for the 6-group structure, in red for the 50 individual precursor structure and in green for the 40 individual precursor structure. In this case it can be seen that the neutron flux as a function of time obtained when using 40 individual precursors diverges from the previous results. This is because by removing the 10 most important precursors the number of delayed neutrons emitted decreases, thus the period of the fissile system decreases. This larger deviation from criticality when 40 precursors are used as β-delayed emitters, can be quantified by calculating the fitted reactivity. In fact, the value for the reactivity was $\rho_{40} = 0.00111(2)$, showing that this system is no longer slightly supercritical, but supercritical. A summary of results obtained can be seen in Table 7, where results for the 6-group and 50 individual precursor structures are also shown for completeness.

6. Summary and conclusions

This work presented the methodology to include the time dependence related to β-delayed neutron emission from individual precursors in the Monte Carlo code OpenMC. This modified code was denominated OpenMC(TD) or Time-Dependent OpenMC. Related to the β-delayed neutron emission, features implemented in OpenMC(TD) were: neutron time labeling and tracking, monitoring of time dependent tallies in the simulation, division of total simulation time in time intervals, a new *precursor* particle, forced decay of precursors in each time interval, population control at the end of each time interval using the combing method and transient source routine to initialize transient simulations. As for the delayed emission from individual precursors in OpenMC(TD), it was included: individual precursor properties from nuclear databases were included in a quantity called importance, grouped or individual precursor treatment, and the capability to perform criticality calculations using individual precursors. To test OpenMC(TD) and to approach the transient modeling of neutron transport in a experimental nuclear reactor, a fissile system was simulated. Different observables obtained with OpenMC(TD) such as reactivity ρ, effective delayed neutron fraction β_{eff}, and prompt generation time Λ, where compared with calculated results, either with exact point kinetic solutions or asymptotic decay constant α_D.

In the case of the monoenergetic system with 1-group precursor structure, differences between OpenMC(TD) and the compared results using point kinetics equations were within the error of the point kinetics result.

In the case of the energy dependent ^{235}U system, total simulation time was 100 μs, with time intervals of 100 ns, describing neutron flux prompt changes (prompt drop or prompt jump for the subcritical or supercritical configuration, respectively) within the first 10μs. Both total simulation time and time interval chosen for these cases were adequate to properly describe the neutron flux transient behaviour in these systems.

In the case of the light-water moderated energy dependent ^{235}U system, criticality calculation shows that it is a slightly supercritical system. The effective multiplication factors obtained using the 6-group structure and 50 individual precursors are in good agreement with each other. Regarding the transient calculations, results obtained using 6-group and 50 individual precursors show a slightly supercritical system, which is consistent with the previous criticality calculation. When the same system is simulated, but with the 10 most important precursors removed, the fitted reactivity shows a supercritical system, due to the decrease of the period of the fissile system.

Regarding the improvement of results, this can be achieved by running longer simulation times, by applying to computing time in a supercomputer facility or by implementing a branchless fission scheme in OpenMC(TD). Nevertheless, OpenMC(TD) has the potential as a Monte Carlo tool to explore how precursor data from nuclear databases impacts on results obtained in fissile systems. In that sense, OpenMC(TD) could become a reliable tool to prompt new experimental data on individual β-delayed neutron emitters.

Declaration of competing interest

The authors declare that they have no known competing financial interests or personal relationships that could have appeared to influence the work reported in this paper.

Acknowledgments

J. Romero-Barrientos acknowledges support from Programa Nacional de Becas de Postgrado under grant 21151413. F. Molina acknowledges support from ANID FONDECYT Regular Project 1171467, ANID FONDECYT Regular Project 1221364, and ANID - Millennium Science Initiative Program - ICN2019_044.

References

[1] G. Keepin, T. Wimett, R. Zeigler, Delayed neutrons from fissionable isotopes of uranium, plutonium and thorium, Journal of Nuclear Energy 6 (1) (1954), https://doi.org/10.1016/0891-3919(57)90178-X (1957) 2 – 21, http://www.sciencedirect.com/science/article/pii/089139195790178X.

[2] D. Brown, et al., ENDF/B-VIII.0: the 8th Major Release of the Nuclear Reaction Data Library with CIELO-Project Cross Sections, New Standards and Thermal Scattering Data, Nuclear Data Sheets 148, 2018, pp. 1–142, https://doi.org/10.1016/j.nds.2018.02.001. , special Issue on Nuclear Reaction Data, http://www.sciencedirect.com/science/article/pii/S0090375218300206.

[3] P. Dimitriou, I. Dillmann, B. Singh, V. Piksaikin, K. Rykaczewski, J. Tain, A. Algora, K. Banerjee, I. Borzov, D. Cano-Ott, S. Chiba, M. Fallot, D. Foligno, R. Grzywacz, X. Huang, T. Marketin, F. Minato, G. Mukherjee, B. Rasco, A. Sonzogni, M. Verpelli, A. Egorov, M. Estienne, L. Giot, D. Gremyachkin, M. Madurga, E. McCutchan, E. Mendoza, K. Mitrofanov, M. Narbonne, P. Romojaro, A. Sanchez-Caballero, N. Scielzo, Development of a reference database for beta-delayed neutron emission, Nuclear Data Sheets 173 (2021) 144–238, https://doi.org/10.1016/j.nds.2021.04.006. , special Issue on Nuclear Reaction Data, https://www.sciencedirect.com/science/article/pii/S0090375221000168.

[4] International Atomic Energy Agency, IAEA CRP on a Reference Database for Beta-Delayed Neutron Emission, 2017. https://www-nds.iaea.org/beta-delayed-neutron/.

[5] P.K. Romano, et al., OpenMC: a state-of-the-art Monte Carlo code for research and development, Annals of Nuclear Energy 82 (2015) 90–97, https://doi.org/10.1016/j.anucene.2014.07.048. , joint International Conference on Supercomputing in Nuclear Applications and Monte Carlo 2013, http://www.sciencedirect.com/science/article/pii/S030645491400379X.

[6] J. Romero-Barrientos, Time-dependent Monte Carlo in Fissile Systems with Beta-Delayed Neutron Precursors, Ph.D. thesis, 2021. arXiv:2101.09338.

[7] J. Romero-Barrientos, Time-dependent Monte Carlo in Fissile Systems with Beta-Delayed Neutron Precursors, Ph.D. thesis, Universidad de Chile, 2022. URL, https://repositorio.uchile.cl/handle/2250/184722.

[8] K.-L. Kratz, Relevance of beta-delayed neutron data for reactor, nuclear physics and astrophysics applications, AIP Conference Proceedings 1645 (1) (2015) 109–120, https://doi.org/10.1063/1.4909565, arXiv:https://aip.scitation.org/doi/pdf/10.1063/1.4909565, https://aip.scitation.org/doi/abs/10.

1063/1.4909565.
[9] Proceedings of the consultants meeting on delayed neutron properties. URL https://www-nds.iaea.org/publications/indc/indc-nds-0107.pdf.
[10] B.L. Sjenitzer, J.E. Hoogenboom, Dynamic Monte Carlo method for nuclear reactor kinetics calculations, Nuclear Science and Engineering 175 (1) (2013) 94–107, arXiv:https://doi.org/10.13182/NSE12-44, doi:10.13182/NSE12-44. URL https://doi.org/10.13182/NSE12-44.
[11] M.C. Brady, Evaluation and Application of Delayed Neutron Precursor Data, Ph.D. thesis, Los Alamos National Laboratory, United States, 4 1989, https://doi.org/10.2172/6187550.
[12] S. Koranne, Hierarchical Data Format 5 : HDF5, Springer US, Boston, MA, 2011, pp. 191–200, https://doi.org/10.1007/978-1-4419-7719-9_10.
[13] R. Macfarlane, D.W. Muir, R.M. Boicourt, A.C. Kahler III, J.L. Conlin, The NJOY Nuclear Data Processing System, Version, Technical Report Los Alamos National Laboratory, 2016, https://doi.org/10.2172/1338791. TRN: US1701456.
[14] K.S. Chaudri, S.M. Mirza, Burnup dependent Monte Carlo neutron physics calculations of IAEA MTR benchmark, Progress in Nuclear Energy 81 (2015) 43–52, https://doi.org/10.1016/j.pnucene.2014.12.018.
[15] J. Chen, L. Cao, C. Zhao, Z. Liu, Development of Subchannel Code SUBSC for high-fidelity multi-physics coupling application, Energy Procedia 127 (2017) 264–274, https://doi.org/10.1016/j.egypro.2017.08.121, international Youth Nuclear Congress 2016, IYNC2016, 24-30 July 2016, Hangzhou, China.
[16] J.-Y. Li, L. Gu, H.-S. Xu, N. Korepanova, R. Yu, Y.-L. Zhu, C.-P. Qin, CAD modeling study on FLUKA and OpenMC for accelerator driven system simulation, Annals of Nuclear Energy 114 (2018) 329–341, https://doi.org/10.1016/j.anucene.2017.12.050.
[17] I. Variansyah, B.R. Betzler, W.R. Martin, Multigroup constant calculation with static α-eigenvalue Monte Carlo for time-dependent neutron transport simulations, Nuclear Science and Engineering 194 (11) (2020) 1025–1043, https://doi.org/10.1080/00295639.2020.1743578.
[18] J.A. Walsh, B. Forget, K.S. Smith, F.B. Brown, On-the-fly Doppler broadening of unresolved resonance region cross sections, Progress in Nuclear Energy 101 (2017) 444–460, https://doi.org/10.1016/j.pnucene.2017.05.032, special Issue on the Physics of Reactors International Conference PHYSOR 2016: Unifying Theory and Experiments in the 21st Century.
[19] J.A. Walsh, P.K. Romano, B. Forget, K.S. Smith, Optimizations of the energy grid search algorithm in continuous-energy Monte Carlo particle transport codes, Computer Physics Communications 196 (2015) 134–142, https://doi.org/10.1016/j.cpc.2015.05.025.
[20] P.K. Romano, A.R. Siegel, B. Forget, K. Smith, Data decomposition of Monte Carlo particle transport simulations via tally servers, Journal of Computational Physics 252 (2013) 20–36, https://doi.org/10.1016/j.jcp.2013.06.011.
[21] B. Zhang, X. Yuan, Y. Zhang, H. Tang, L. Cao, Development of a versatile depletion code AMAC, Annals of Nuclear Energy 143 (2020), 107446, https://doi.org/10.1016/j.anucene.2020.107446.
[22] X. Peng, J. Liang, B. Forget, K. Smith, Calculation of adjoint-weighted reactor kinetics parameters in OpenMC, Annals of Nuclear Energy 128 (2019) 231–235, https://doi.org/10.1016/j.anucene.2019.01.007.
[23] J. Romero-Barrientos, J.M. Damián, F. Molina, M. Zambra, P. Aguilera, F. López-Usquiano, B. Parra, A. Ruiz, Calculation of kinetic parameters β_{eff} and λ with modified open source Monte Carlo code openmc(td), Nuclear Engineering and Technology 54 (3) (2022) 811–816, https://doi.org/10.1016/j.net.2021.09.020. URL, https://www.sciencedirect.com/science/article/pii/S1738573321005623. URL.
[24] D. Foligno, New Evaluation of Delayed-Neutron Data and Associated Covariances, Ph.D. thesis, Aix Marseille Université, 2020.
[25] M. Kellett, O. Kellett, R. Mills, JEFF Report 20: the JEFF-3.1/-3.1.1 Radioactive Decay Data and Fission Yields Sub-libraries, 2009.
[26] D. Legrady, J.E. Hoogenboom, Scouting the feasability of Monte Carlo reactor dynamics simulations, International Conference on the Physics of Nuclear Reactors (2008) 1–5.
[27] T. Booth, A Weight (Charge) Conserving Importance-Weighted Comb for Monte Carlo, Conference: American Nuclear Society (ANS) Radiation Protection and Shielding Division Topical Meeting on Advancements and Applications in Radiation Protection and Shielding (TRN: 96:002172).
[28] D. Legrady, M. Halasz, J. Kophazi, B. Molnar, G. Tolnai, Population-based variance reduction for dynamic Monte Carlo, Annals of Nuclear Energy 149 (2020) 107752. doi:https://doi.org/10.1016/j.anucene.2020.107752. URL {https://www.sciencedirect.com/science/article/pii/S0306454920304503}.
[29] B. Molnar, G. Tolnai, D. Legrady, A GPU-based direct Monte Carlo simulation of time dependence in nuclear reactors, Annals of Nuclear Energy 132 (2019) 46–63, https://doi.org/10.1016/j.anucene.2019.03.024. URL, https://www.sciencedirect.com/science/article/pii/S0306454919301495.
[30] C. de Mulatier, E. Dumonteil, A. Rosso, A. Zoia, The critical catastrophe revisited, Journal of Statistical Mechanics: Theory and Experiment (2015), P08021, https://doi.org/10.1088/2F1742-5468/2F2015/2F08/2Fp08021.
[31] International Evaluation of Neutron Cross-Section Standards, International Atomic Energy Agency, Vienna, 2007. URL, https://www.iaea.org/publications/7653/international-evaluation-of-neutron-cross-section-standards.